J. Chem. Sci. Vol. 129, No. 11, November 2017, pp. 1687–1693.
https://doi.org/10.1007/s12039-017-1369-0

REGULAR ARTICLE

Special Issue on RECENT TRENDS IN THE DESIGN & DEVELOPMENT OF CATALYSTS AND THEIR APPLICATION

Enhancement of visible light irradiation photocatalytic activity of $SrTiO_3$ nanoparticles by Pt doping for oxidation of cyclohexane

MOHAMED ABDEL SALAM[a,*] and HIND AL-JOHANI[b]

[a]Chemistry Department, Faculty of Science, King Abdulaziz University, P.O. Box 80200, Jeddah 21589, Saudi Arabia
[b]Chemistry Department, College of Alwajh, University of Tabuk, Al Wajh, Saudi Arabia
E-mail: masalam16@hotmail.com

MS received 15 March 2017; revised 13 July 2017; accepted 5 August 2017; published online 25 September 2017

Abstract. In this research, strontium titanate ($SrTiO_3$) nanoparticles were synthesised using an ultrasonic method, then were doped with Pt using a photo-assisted deposition method to form Pt/$SrTiO_3$ nanoparticles. $SrTiO_3$ and Pt/$SrTiO_3$ nanoparticles were characterized by XRD, XPS, TEM, BET surface area UV–Vis and PL techniques in order to explore their chemical and physical properties. The visible light irradiation photocatalytic performances of $SrTiO_3$ nanoparticles and Pt/$SrTiO_3$ nanoparticles for photocatalytic oxidation of cyclohexane was investigated, and the results revealed that platinum was doped onto the $SrTiO_3$ nanoparticles surfaces as metallic platinum, and the weight percent of doped platinum greatly affected the band gap, and the 1.5 wt% Pt/$SrTiO_3$ nanoparticles showed the highest photocatalytic activity due to the low band gap. The stability of the Pt/$SrTiO_3$ nanoparticles for the photocatalytic oxidation of cyclohexane was examined and the results revealed that the Pt/$SrTiO_3$ nanoparticles could be used five times without losing their efficiency.

Keywords. $SrTiO_3$; Pt doping; photocatalytic; oxidation; cyclohexane.

1. Introduction

Oil and natural gas contain many different compounds and the most abundant ones are hydrocarbons, especially alkanes. One of the main advantages of alkanes is that they can be used as a precursor to many other chemicals. For example, alkanes could be oxidized selectively and can be used to produce more important chemicals that can further be used in different applications. This selective oxidation reaction is one of the major processes for the production of KA-oil; a mixture of cyclohexanol and cyclohexanone, which could be produced by the selective oxidation of cyclohexane.[1,2] KA-oil is considered as an important intermediate chemical in many petroleum industrial chemistry for the production of different polymers such as nylon.[3] Therefore, the selective oxidation of cyclohexane is considered to be of great importance for scientific and industrial applications. Nevertheless, the selective oxidation of cyclohexane in the industry is an expensive process because it requires the application of high temperature and pressure, which in turn consumes large amounts of energy. In addition, undesired by-products such as toluene, methyl-cyclohexane, heptene, 1-hexene, and 5-hexanal are produced during the oxidation process, which makes the recovery/separation steps more difficult and lowers the product yield as well.[4] Currently, scientific communities all around the globe are focused on the development of highly selective and efficient method for the selective oxidation of cyclohexane. One of the possible alternatives for the energy intensive oxidation of cyclohexane is photocatalysis, which is widely applied in different fields for the production of chemicals,[5] for water remediation[6] and air.[7] Transition metal oxides and semiconductors are commonly used as heterogeneous photocatalysts due to their unique characteristics.[8] Currently, there are few studies devoted to the development of photocatalysts for organic synthesis via the selective oxidation of alkanes.[9–11] The development of novel and efficient photocatalysts for the selective oxidation of cyclohexane is the focus of many research scientists, however, the resulting photocatalysts often suffer from different problems such as the lower efficiency, and from a positive impact on charge recombination, which affects the catalytic performance.

$SrTiO_3$ is an oxide semiconductor and is considered as a promising photocatalyst for different processes.[12–16]

*For correspondence

Many research works showed the possibility of enhancing the photocatalytic activity of $SrTiO_3$ in the visible light region by doping it with other metal or metal oxides. For example, doping $SrTiO_3$ with Rh greatly enhanced the catalytic properties of $SrTiO_3$ photocatalyst for efficient hydrogen production;[17] doping $SrTiO_3$ with Cr greatly enhanced their photocatalytic activity for the visible-light-driven transformation of CO_2 into CH_4;[18] doping $SrTiO_3$ with TiO_2 and nitrogen for the synthesis of macroporous monolithic photocatalyst were used efficiently for the photodegradation of Rhodamine B organic dye under visible light.[19] It was also observed that doping $SrTiO_3$ with Bi_2O_3 and the construction of heterojunction significantly improved the photocatalytic activity of $SrTiO_3$ for tetracycline degradation under visible light,[20] the preparation of $BiVO_4/SrTiO_3$ composite greatly enhanced the photocatalytic degradation of the antibiotic sulfamethoxazole under sunlight.[21] Also, it is well-known that doping different photocatalysts with Pt significantly enhances their photocatalytic activities. For example, doping Al_2O_3, TiO_2 and ZrO_2 with Pt greatly enhanced their activities for the oxidation of cyclohexane to cyclohexanone and cyclohexanol.[22] Also, doping $AgInS_2$ nanoparticles with Pt significantly enhanced their activity for the photocatalytic oxidation of cyanide in water under visible light,[23] whereas the photocatalytic reduction of CO_2 to CH_4 could be enhanced by doping TiO_2 nanoparticles[24] and graphitic carbon nitride (g-C_3N_4)[25] by Pt.

In this research study, $SrTiO_3$ nanoparticles were prepared and then doped with platinum metal to form a novel photocatalyst; $Pt/SrTiO_3$ nanoparticles, which were then used for the selective photocatalytic oxidation of cyclohexane using visible light irradiation. The $SrTiO_3$and $Pt/SrTiO_3$ nanoparticles were characterized by XRD, XPS, TEM, BET surface area UV–Vis, and PL techniques to clarify the formation of the $SrTiO_3$ nanoparticles, the dispersion of the Pt over the $SrTiO_3$, and the formation of stable $Pt/SrTiO_3$ nanoparticles. Also, the stability of the $Pt/SrTiO_3$ nanoparticles for the photocatalytic oxidation of cyclohexane was investigated.

2. Experiment

2.1 *Photocatalysts preparation*

$SrTiO_3$ nanoparticles are prepared by an ultrasonic method. 0.3 mole of strontium acetate was added under a nitrogen atmosphere to 16 mol of glacial acetic acid and stirred for 2 h at room temperature. Then, 5 mol of titanium isopropoxide was added to the solution mentioned above and the resulting mixture was stirred at room temperature for 6 h. Then, 20 mL of acetone was added and the resulting mixture was put in an apparatus for low-frequency ultrasound (Bransonic 42 kHz) for 1 h. The resulting materials were dried for 24 h at 100°C, and then the materials were calcined at 550°C for 5 h in air. A photo-assisted deposition (PAD) route was used to prepare $Pt/SrTiO_3$ samples which contain different wt% from Pt metal (0.5, 1.0, 1.5 and 2.0 wt%). In this route, Pt metal was deposited on $SrTiO_3$ under UV-light irradiation by using an aqueous solution of platinum chloride. The obtained samples dried for 24 h at 60°C and treated via H_2 reduction (20 mL min^{-1}) at 60°C for 2 h.

2.2 *Photocatalysts characterization*

The crystalline phase of the $SrTiO_3$ and $Pt/SrTiO_3$ nanoparticles was determined using powder X-ray diffraction (XRD), Bruker axis D8 instrument using CuK_α radiation (λ = 1.540 Å) in the 2θ range from 10° to 80° at room temperature. The chemical state information of the nanoparticles was determined using X-ray photoelectron spectroscopy (XPS); Thermo Scientific K-ALPHA spectrometer. The morphological structure of the $SrTiO_3$and $Pt/SrTiO_3$ nanoparticles were examined using a transmission electron microscope (TEM); JEOL-JEM-1230. Specimens for TEM analyses were prepared by dispersing the nanoparticles in ethanol and placing one drop onto a holey-carbon-coated copper supported grid. The specific surface area was determined from nitrogen adsorption/desorption isotherms which were measured at 77 K by using a Nova 2000 series Chromatech. Prior to the analysis, the samples were outgassed at 150°C for 24 h. UV–Vis–NIR spectrophotometer (V-570, Jasco, Japan) was used to estimate the band gap in the air at room temperature to detect absorption over the range of 200 to 800 nm based on the ultra violet-visible diffuse reflectance spectra (UV–Vis-DRS) using a standard cell for solid materials from Jasco, Japan. Shimadzu RF-5301 fluorescence spectrophotometer was used to measure the photoluminescence emission spectra (PL) of the nanoparticles.

2.3 *Photocatalytic oxidation of cyclohexane*

Photocatalytic experiments were performed by feeding 30 L/h (STP) N_2 stream containing 200 ppm cyclohexane, 10 vol.% O_2 and adding 320 ppm of water at 60°C in order to minimize catalysts photodeactivation, and the reaction pressure was 1 atm. Nitrogen was the carrier gas for cyclohexane and water vaporized from 60°C controlled saturators, and a fluidized bed photoreactor was used. The reactor was irradiated by a Xenon lamp with 300 W power and 0.96 W/cm^2 intensity covered by a cut-off filter of 420 nm. The catalytic bed was composed of 1.2 g of catalyst mixed with 20 g glass spheres in order to improve the fluidization properties. The reactor inlet reactants and outlet products were analyzed using gas chromatography Agilent GC 7890A model. The reactor was irradiated

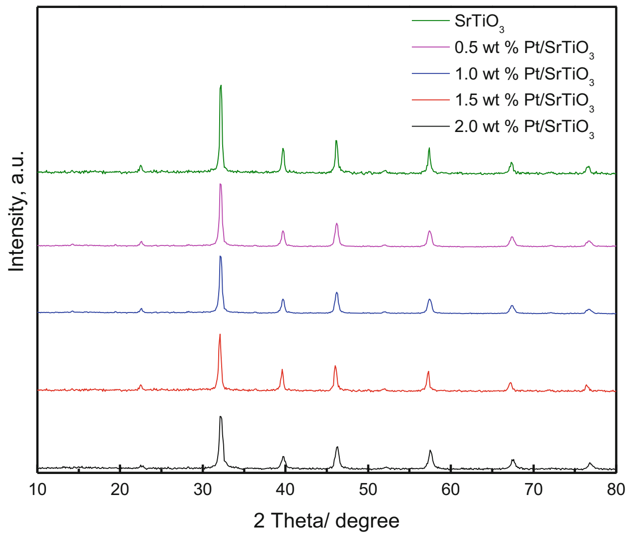

Figure 1. XRD patterns of $SrTiO_3$ and $Pt/SrTiO_3$ nanoparticles.

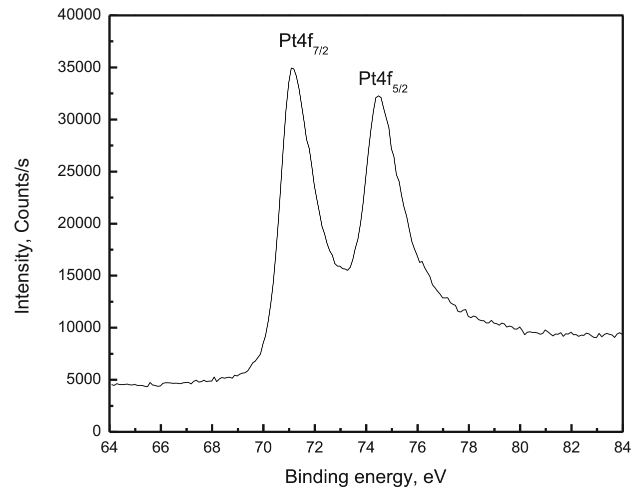

Figure 2. XPS spectra of Pt 4f of 1.5 wt% $Pt/SrTiO_3$ nanoparticle.

after complete adsorption of cyclohexane on the catalyst surface.

The photocatalytic behavior of all analyzed samples was evaluated as:

$$X = (C_0 - C_t)/C_0 \times 100$$

where X = cyclohexane conversion; C_0 = inlet cyclohexane concentration and C_t = outlet cyclohexane concentration.

3. Results and Discussion

3.1 *Characterization of $SrTiO_3$ and $Pt/SrTiO_3$ nanoparticles*

Figure 1 illustrated the XRD patterns of the $SrTiO_3$and $Pt/SrTiO_3$ nanoparticles. The results revealed that the $SrTiO_3$ and $Pt/SrTiO_3$ nanoparticles XRD patterns had the characteristic peaks of $SrTiO_3$, suggesting that the doping $SrTiO_3$nanoparticles with Pt do not significantly affect their structure. Furthermore, the characteristic XRD peaks for platinum or platinum oxide were not detected, which could be attributed to the fact that the weight percent platinum was lower than the XRD detection limit and/or the good dispersion of the Pt on the $SrTiO_3$nanoparticle surfaces. The same phenomenon was observed when oxomolybdate species were dispersed over TiO_2 and were used for direct methanol oxidation.[26]

Also, it was observed that the characteristic $SrTiO_3$ peak intensities decreased as the weight percent of doped platinum increases, especially at 32.15°. Scherer equation was used to calculate the $SrTiO_3$ crystallite size based on the half-width of the most intense peak at $2\theta = 32.15°$. The crystallite size values were 24.0, 20.0, 17.0,14 and 12.0 nm for $SrTiO_3$, 0.5 wt% $Pt/SrTiO_3$, 1.5 wt% $Pt/SrTiO_3$ and 2.0 wt% $Pt/SrTiO_3$, respectively, indicating that Pt doping on the $SrTiO_3$ surface decreases the $SrTiO_3$ crystallite size due to the degradation of crystallinity as a result of local distortion of the crystal structure.[27,28]

The XPS spectra of Pt 4f of 1.5 wt% $Pt/SrTiO_3$ nanoparticle are shown in Figure 2. The results demonstrated that the presence of two peaks of Pt 4f at a binding energy equal to 70.3 and 74.0 eV confirms the presence of metallic platinum,[29] as shown in Figure 2.

Figure 3 shows the TEM images of $SrTiO_3$ and 1.5 wt % $Pt/SrTiO_3$ nanoparticles. These images demonstrate that $SrTiO_3$ is a spherical nanoparticle as shown in Figure 3a and that platinum was doped as dots as shown in Figure 3b.

Table 1 shows the BET specific surface area of the $SrTiO_3$ and $Pt/SrTiO_3$ nanoparticles which was calculated according to the BET adsorption isotherm model.[30] The BET surface area values were 20, 18, 16, 14 and 10 m^2/g for $SrTiO_3$, 0.5 wt % $Pt/SrTiO_3$, 1.5 wt % $Pt/SrTiO_3$, and 2.0 wt % $Pt/SrTiO_3$, respectively. The BET surface area values of the $Pt/SrTiO_3$ nanoparticles were lower than those of the $SrTiO_3$ nanoparticles, which could be attributed to the blocking of $SrTiO_3$ nanoparticles pores with the Pt nanoparticles upon the doping process.

Figure 4 demonstrated the UV–Vis-DRS of the $SrTiO_3$ and $Pt/SrTiO_3$ nanoparticles. The results revealed that the $SrTiO_3$ nanoparticles are absorbed in the UV region, and upon doping with Pt nanoparticles, in general, the absorption peaks were shifted; 368 nm, 375 nm, 373 nm, 370 nm, and 366 nm for $SrTiO_3$, 0.5

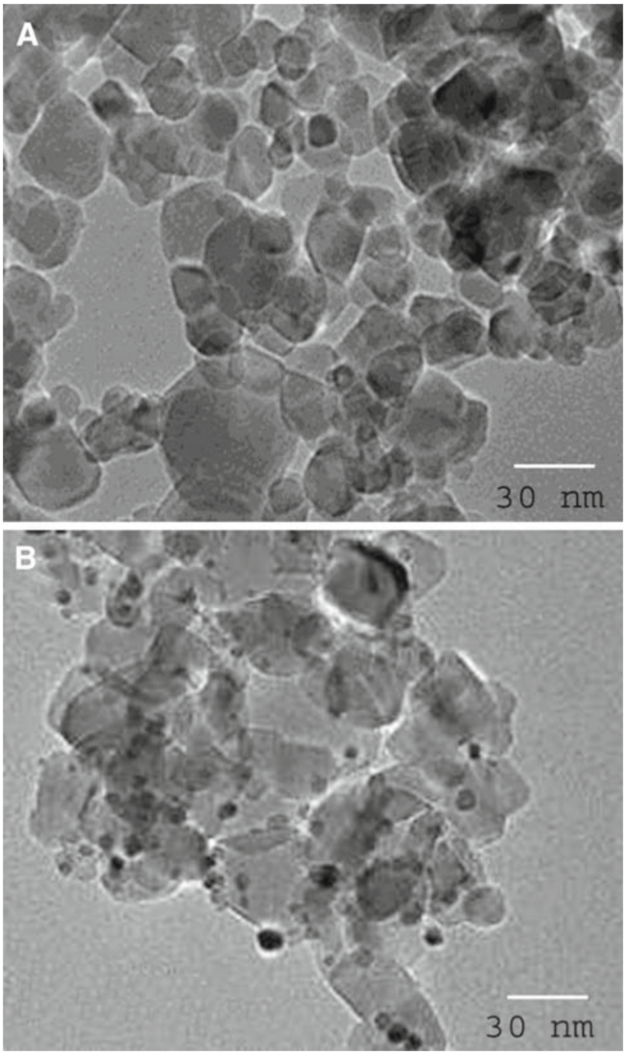

Figure 3. TEM images of $SrTiO_3$ (**a**) and 1.5 wt% $Pt/SrTiO_3$ (**b**) nanoparticles.

Table 1. BET surface area of $SrTiO_3$ and Pt- doped $SrTiO_3$ nanoparticles.

Sample	S_{BET} (m^2/g)
$SrTiO_3$	20
0.5 wt% Pt doped $SrTiO_3$	18
1.0 wt% Pt doped $SrTiO_3$	16
1.5 wt% Pt doped $SrTiO_3$	14
2.0 wt% Pt doped $SrTiO_3$	10

wt% $Pt/SrTiO_3$, 1.5 wt% $Pt/SrTiO_3$, and 2.0 wt% $Pt/SrTiO_3$, respectively, which was observed earlier when titania nanotubes were doped with Pt.[31] The band gap (E_g) for the $SrTiO_3$ and $Pt/SrTiO_3$ nanoparticles was calculated from the UV–Vis–DRS by using Tauc's relation:[32]

$$\alpha h\nu = B(h\nu - E_g)^n$$

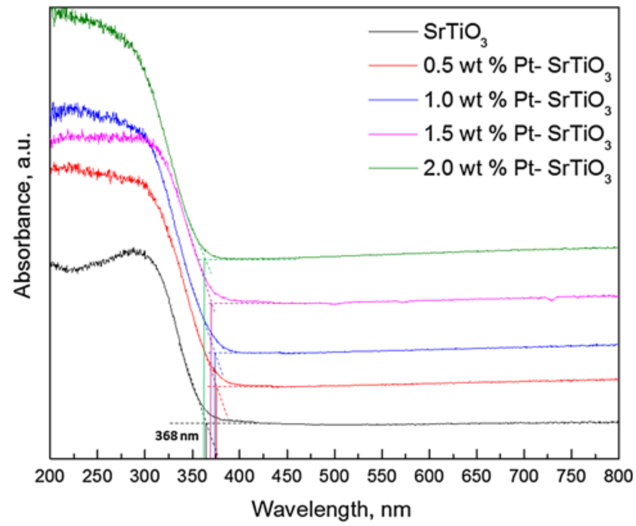

Figure 4. UV–Vis absorption spectra of $SrTiO_3$ and $Pt/SrTiO_3$ nanoparticles.

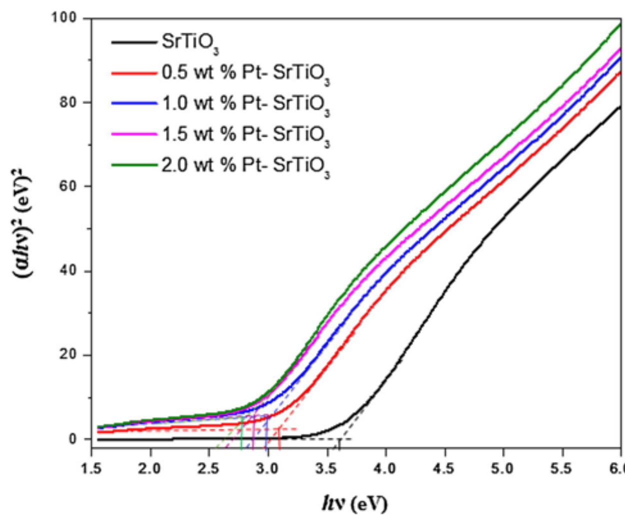

Figure 5. Band gap energy calculations for $SrTiO_3$ and $Pt–SrTiO_3$ samples.

where α is the optical absorption coefficient, E (= hc/λ) is the photon energy, B is a constant, λ is the measured wavelength in nm, Eg is the optical band gap and n is 1/2 or 2 for direct or indirect band gap semiconductor, respectively. Figure 5 showed the linear part of the plot of $(\alpha h \nu)^2$ vs. α h, and the E_g values were estimated by extrapolating each plot to its baseline, and their values were presented in Table 2. It is clear that the band gap energy values for the doped samples are smaller than those for the pure one, and the $SrTiO_3$ band gap can be controlled by the doped Pt weight percent.

Figure 6 illustrates the PL spectra of the $SrTiO_3$ and $Pt/SrTiO_3$ nanoparticles. The results showed that the peak intensity of the PL for the $SrTiO_3$ was reduced as the Pt weight percent increased from 0.0 to 1.5, and

Table 2. Band gap energies of $SrTiO_3$ and Pt-doped $SrTiO_3$ nanoparticles.

Sample	Band gap energy eV
$SrTiO_3$	3.60
0.5 wt% Pt doped $SrTiO_3$	3.10
1.0 wt% Pt doped $SrTiO_3$	2.98
1.5 wt% Pt doped $SrTiO_3$	2.85
2.0 wt% Pt doped $SrTiO_3$	2.75

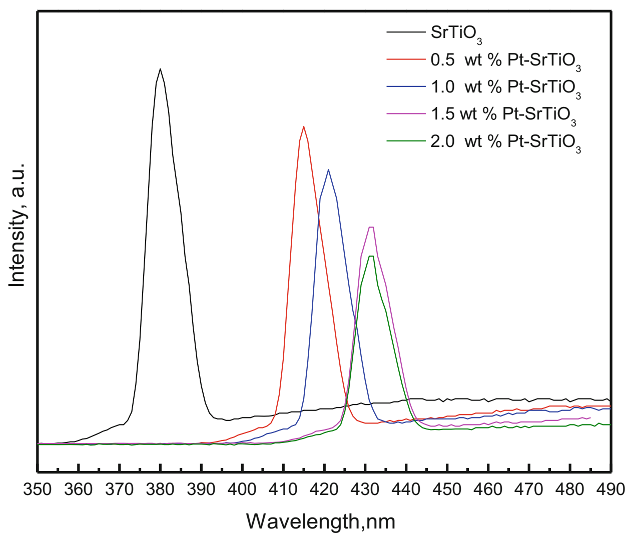

Figure 6. PL spectra of $SrTiO_3$ and $Pt/SrTiO_3$ nanoparticles (the excitation wavelength is 280 nm).

at a Pt weight percent greater than 1.5 did not affect the PL peak intensity, indicating the significant effect of doping $SrTiO_3$ with Pt, which influences the rate of the electron-hole recombination. This may be due to Pt nanoparticles which lead to the formation of Schottky barriers on the $SrTiO_3$, and work as electron traps. These electron traps facilitated the electron–hole separation and promotes the interfacial electron transfer process, which accordingly, make the photocatalyst more efficient.[33]

3.2 *Photocatalytic oxidation of cyclohexane*

Figure 7 shows the effect of the doped Pt weight percent on the photocatalytic activities of $SrTiO_3$ nanoparticles for photocatalytic oxidation of cyclohexane. The results showed that the photocatalytic activity was significantly enhanced, 5.0%, 75%, 85%, 100% with the increase of doped Pt weight percent from 0.0, 0.5, 1.0, 1.5 wt%; respectively, which was expected due to the doping with noble metal such as Pt.[34] Moreover, the photocatalytic activity did not change with increase in the

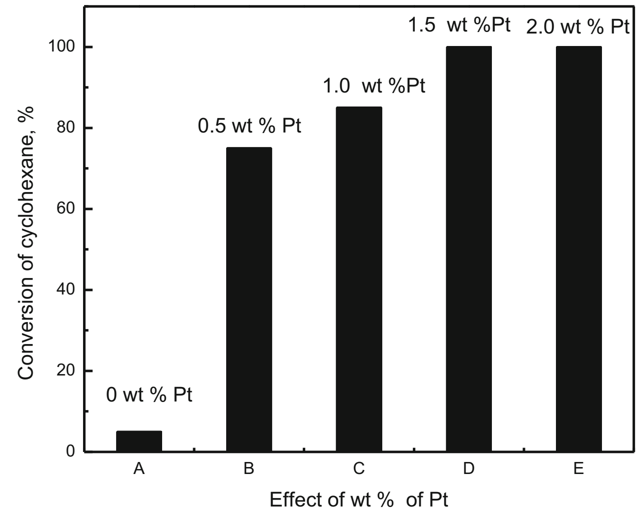

Figure 7. Effect of the doped platinum weight percent on the photocatalytic activity of $SrTiO_3$ nanoparticles for photocatalytic oxidation of cyclohexane.

doped metallic Pt weight percent above 1.5 wt%. Therefore, the doped metallic Pt weight percent affect the electron-hole recombination rate of $SrTiO_3$ nanoparticles and band gap. Accordingly, it can be concluded that 1.5 wt% $Pt/SrTiO_3$ nanoparticles showed the uppermost photocatalytic activity, lowest electron-hole recombination rate and band gap.

The stability of the $Pt/SrTiO_3$ nanoparticles for the photocatalytic oxidation of cyclohexane was investigated using the 1.5 wt% $Pt/SrTiO_3$ nanoparticles and the results showed that 1.5 wt% $Pt/SrTiO_3$ nanoparticles had a high photocatalytic stability after being used for five successive times, which is a common practice to verify the $Pt/SrTiO_3$ nanoparticles stability.[35]

Accordingly, the enhancement of the catalytic activity of the doped $Pt/SrTiO_3$ photocatalyst compared to the prepared $SrTiO_3$ photocatalyst could be due to many reasons. First, the prevention of the recombination of the electron-hole pair by Pt atoms in the $Pt/SrTiO_3$ photocatalyst, as the doped metal atoms often act as electron traps,[36] second; the decrease of band gap energy that allows absorption of photons in the visible region, and finally the promotion of the interfacial electron transfer process as the Pt nanoparticles lead to formation of Schottky barriers on the $SrTiO_3$, and work as electron traps, which facilitate the electron–hole separation.

4. Conclusions

$SrTiO_3$ nanoparticles were prepared and were then doped with different weight percent of Pt metal using the photoassisted deposition method. The XRD measurements showed the characteristic peak of the $SrTiO_3$ nanoparticles with the absence of the Pt characteristic peaks due to the low weight percent and the good dispersion of the Pt over the $SrTiO_3$ nanoparticles. Also, Pt doping on the $SrTiO_3$ surface decreases the $SrTiO_3$ crystallite size. The XPS measurements showed that the doped Pt is present as metallic platinum. Also, Pt doping on $SrTiO_3$ nanoparticles shifts absorption maximum to longer wavelengths. Complete photocatalytic oxidation of cyclohexane was achieved using the 1.5 wt% $Pt/SrTiO_3$ photocatalyst based on a photocatalyst dose of 1.2 g/L, a cyclohexane concentration of 200 ppm and a reaction time of 90 min. The 1.5 wt% $Pt/SrTiO_3$photocatalyst showed high photocatalytic stability after being used for five successive times. The results revealed that 1.5 wt% $Pt/SrTiO_3$ photocatalyst was acknowledged as the most active photocatalyst, and finally, the $Pt/SrTiO_3$ nanoparticles have high photocatalytic activity under visible light for the oxidation of cyclohexane.

Acknowledgements

This work was funded by the Deanship of Scientific Research (DSR), King Abdulaziz University, Jeddah, under Grant No. (130-94-D1435). The authors acknowledge and thank DSR technical and financial support.

References

1. Uruş S, Adıgüzel H and İncesu M 2016 Synthesis of novel N_4O_4 type bis(diazoimine)–metal complexes supported on mesoporous silica: Microwave assisted catalytic oxidation of cyclohexane, cyclooctane, cyclohexene and styrene *Chem. Eng. J.* **296** 90
2. Lončarević D, Krstić J, Dostanić J, Manojlović D, Čupić Ž and Jovanović D M 2010 Cyclohexane oxidation and cyclohexyl hydroperoxide decomposition by poly(4-vinylpyridine-co-divinylbenzene) supported cobalt and chromium complexes *Chem. Eng. J.* **157** 181
3. Silva A R, Mourão T and Rocha J 2013 Oxidation of cyclohexane by transition-metal complexes with biomimetic ligands *Catal. Today* **203** 81
4. Liu S, Liu Z and Kawi S 1998 Liquid-phase oxidation of cyclohexane using Co-P-MCM-41 catalyst *Korean J. Chem. Eng.* **15** 510
5. Chen J, Cen J, Xu X and Li X 2016 The application of heterogeneous visible light photocatalysts in organic synthesis *Catal. Sci. Technol.* **6** 349
6. Lee S-Y and Park S-J 2013 TiO_2 Photocatalyst for water treatment applications *J. Ind. Eng. Chem.* **19** 1761
7. Luengas A, Barona A, Hort C, Gallastegui G, Platel V and Elias A 2015 A review of indoor air treatment technologies *Rev. Environ. Sci. Biotechnol.* **14** 499
8. Litter M I 1999 Heterogeneous photocatalysis: Transition metal ions in photocatalytic systems *Appl. Catal. B* **23** 89
9. Carneiro J T, Yang C-C, Moulijn J A and Mul G 2011 The effect of water on the performance of TiO_2 in photocatalytic selective alkane oxidation *J. Catal.* **277** 129
10. Zhong W, Qiao T, Dai J, Mao L, Xu Q, Zou G, Liu X, Yin D and Zhao F 2015 Visible-light-responsive sulfated vanadium-doped TS-1 with hollow structure: Enhanced photocatalytic activity in selective oxidation of cyclohexane *J. Catal.* **330** 208
11. Kim J, Ichikuni N, Hara T and Shimazu S 2016 Study on the selectivity of propane photo-oxidation reaction on SBA-15 supported Mo oxide catalyst *Catal. Today* **265** 90
12. Yu K, Zhang C, Chang Y, Feng Y, Yang Z, Yang T, Lou L-L and Liu S 2017 Novel three-dimensionally ordered macroporous $SrTiO_3$ photocatalysts with remarkably enhanced hydrogen production performance *Appl. Catal. B* **200** 514
13. He G-L, Zhong Y-H, Chen M-J, Li X, Fang Y-P and Xu Y-H 2016 One-pot hydrothermal synthesis of $SrTiO_3$-reduced graphene oxide composites with enhanced photocatalytic activity for hydrogen production *J. Mol. Catal. A* **423** 70
14. Xu Y and Schoonen M A A 2000 The absolute energy positions of conduction and valence bands of selected semiconducting minerals *Am. Mineral.* **85** 543
15. Yu H, Ouyang S, Yan S, Li Z, Yu T and Zou Z 2011 Sol–gel hydrothermal synthesis of visible-light-driven Cr-doped $SrTiO_3$ for efficient hydrogen production *J. Mater. Chem.* **21** 11347
16. Wang D, Ye J, Kako T and Kimura T 2006 Photophysical and photocatalytic properties of $SrTiO_3$ doped with Cr cations on different sites *J. Phys. Chem. B* **110** 15824
17. Shen P, Lofaro Jr. J C, Woerner W R, White M G, Su D and Orlov A 2013 Photocatalytic activity of hydrogen evolution over Rh doped $SrTiO_3$ prepared by polymerizable complex method *Chem. Eng. J.* **223** 200
18. Bi Y, Ehsan M F, Huang Y, Jin J and He T 2015 Synthesis of Cr-doped $SrTiO_3$ photocatalyst and its application in visible-light-driven transformation of CO_2 into CH_4 *J. CO_2 Util.* **12** 43
19. Ruzimuradov O, Sharipov K, Yarbekov A, Saidov K, Hojamberdiev M, Prasad R M, Cherkashinin G and Riedel R 2015 A facile preparation of dual-phase nitrogen-doped $TiO_2-SrTiO_3$ macroporous monolithic photocatalyst for organic dye photodegradation under visible light *J. Eur. Ceram. Soc.* **35** 1815
20. Che H, Chen J, Huang K, Hu W, Hu H, Liu X, Che G, Liu C and Shi W 2016 Construction of $SrTiO_3/Bi_2O_3$ heterojunction towards to improved separation efficiency of charge carriers and photocatalytic activity under visible light *J. Alloys Compd.* **688** 882
21. Li J, Wang F, Meng L, Han M, Guo Y and Sun C 2017 Controlled synthesis of $BiVO_4/SrTiO_3$ composite with enhanced sunlight-driven photofunctions for sulfamethoxazole removal *J. Colloid Interface Sci.* **485** 116
22. Hammoumraoui I R, Braham A C, Roy L P and Kappenstein C 2011 Catalytic oxidation of cyclohexane to cyclohexanone and cyclohexanol by tert-butyl hydroperoxide over Pt/oxide catalysts *Bull. Mater. Sci.* **34** 1127

23. Azam E S 2014 Photocatalytic oxidation of cyanide under visible light by Pt doped $AgInS_2$ nanoparticles *J. Ind. Eng. Chem.* **20** 4008
24. Xiong Z, Wang H, Xu N, Li H, Fang B, Zhao Y, Zhang J and Zheng C 2015 Photocatalytic reduction of CO_2 on Pt^{2+}–Pt^0/TiO_2 nanoparticles under UV/Vis light irradiation: A combination of Pt^{2+} doping and Pt nanoparticles deposition *J. Hydrogen Energy* **40** 10049
25. Ong W-J, Tan L-L, Chai S-P and Yong S-T 2015 Heterojunction engineering of graphitic carbon nitride (g-C_3N_4) via Pt loading with improved daylight-induced photocatalytic reduction of carbon dioxide to methane *Dalton Trans.* **44** 1249
26. Faye J, Capron M, Takahashi A, Paul S, Katryniok B, Fujitani T and Dumeignil F 2015 Effect of dispersion on to dimethoxymethane over MoOx/TiO_2 *Energy Sci. Eng.* **3** 115
27. Hassan M M, Khan W, Azam A and Naqvi A H 2014 Effect of size reduction on structural and optical properties of ZnO matrix due to successive doping of Fe ions *J. Lumin.* **145** 160
28. Pal M, Pal U, Gracia J M, Jiménez Y and Pérez-Rodríguez F 2012 Effects of crystallization and dopant concentration on the emission behavior of TiO_2:Eu nanophosphors *Nanoscale Res. Lett.* **7**. doi:10.1186/1556-276X-7-1
29. Şen F and Gökagaç G 2007 Different sized platinum nanoparticles supported on carbon: an XPS study on these methanol oxidation catalyst *J. Phys. Chem. C* **111** 5715
30. Brunauer S, Emmett P H and Teller E 1938 Adsorption of gases in multimolecular layers *J. Am. Chem. Soc.* **60** 309
31. Vijayan B K, Dimitrijevic N M, Wu J and Gray K A 2010 The effects of Pt doping on the structure and visible light photoactivity of titania nanotubes *J. Phys. Chem. C* **114** 21262
32. Chrysicopoulou P, Davazoglou D, Trapalis C and Kordas G 1998 Photocatalytic destruction of methylene blue on Ag@TiO_2 with core/shell structure *Thin Solid Films* **323** 188
33. Grabowska E, Marchelek M, Klimczuk T, Lisowski W and Zaleska-Medynska A 2017 TiO_2/$SrTiO_3$ and $SrTiO_3$ microspheres decorated with Rh, Ru or Pt nanoparticles: Highly UV–vis responsible photoactivity and mechanism *J. Catal.* **350** 159
34. Neppolian B, Mine S, Horiuchi Y, Bianchi C L, Matsuoka M, Dionysiou D D and Anpo M 2016 Efficient photocatalytic degradation of organics present in gas and liquid phases using Pt-TiO_2/Zeolite (H-ZSM) *Chemosphere* **153** 237
35. Pol R, Guerrero M, García-Lecina E, Altube A, Rossinyol E, Garroni S, Baró M D, Pons J, Sort J and Pellicer E 2016 Ni-, Pt- and (Ni/Pt)-doped TiO_2 nanophotocatalysts: A smart approach for sustainable degradation of Rhodamine B dye *Appl. Catal. B* **181** 270
36. Mohamed R M, McKinney D L and Sigmund W M 2012 Enhanced nanocatalysts *Mater. Sci. Eng. R* **73** 1